

In vivo laminar electrophysiology co-registered with histology in the hippocampus of patients with temporal lobe epilepsy

István Ulbert,^{a,b,*} Zsófia Maglóczky,^c Loránd Eröss,^d Sándor Czirják,^e János Vajda,^e
László Bognár,^e Szabolcs Tóth,^d Zerind Szabó,^d Péter Halász,^f Dániel Fabó,^f
Eric Halgren,^{b,g} Tamás F. Freund,^c and George Karmos^a

^a*Institute for Psychology of the Hungarian Academy of Sciences, Budapest 1068, Hungary*

^b*Athinoula A. Martinos Center for Biomedical Imaging, Massachusetts General Hospital, Massachusetts Institute of Technology, Harvard Medical School, Charlestown, MA 02129, USA*

^c*Institute of Experimental Medicine of the Hungarian Academy of Sciences, Budapest 1450, Hungary*

^d*Department of Neurosurgery, MÁV Hospital, Budapest 1062, Hungary*

^e*National Institute for Neurosurgery, Budapest 1577, Hungary*

^f*National Institute of Psychiatry and Neurology, Epilepsy Center, Budapest 1021, Hungary*

^g*INSERM, Marseilles, France*

Received 27 August 2003; revised 4 December 2003; accepted 8 December 2003

Available online 10 February 2004

Abstract

Laminar multiple microelectrodes have been developed to sample cortical and hippocampal activity in animals. If these measurements are adequately co-registered with the anatomy of the region, they can yield important information about its function and structure. In vivo laminar electrophysiological recordings from the human epileptic hippocampus are rare. However, histological and immunohistochemical analyses are widely used to determine the structural changes associated with temporal lobe epilepsy (TLE). Here we present data obtained by a combined approach: intraoperative recording of laminar field potentials, single and multiple unit activity under anesthesia, accompanied by histology and immunohistochemistry from the same hippocampal region of epileptic patients undergoing temporal lobectomy for drug-resistant TLE. The stability of the electrophysiology and the accuracy of its co-registration with histology were tested successfully. We have found large field potential spikes associated with bursting single units in CA1. Intracortical and subdural strip recordings from the lateral temporal cortex showed similar field potential activation patterns. A prominent oscillatory activity was present in the dentate gyrus with highly localized field potential gradient and multiple unit activity. This pattern could be used as a landmark defining the position of the electrode in the hippocampus. Our findings indicate that some aspects of the local and network epileptiform activity in the hippocampal formation are likely preserved under anesthesia. Electrophysiological identification of the functional state of the hippocampus together with its local structural correlates could further enhance our understanding of this disease.

© 2004 Elsevier Inc. All rights reserved.

Keywords: Temporal lobe epilepsy; Hippocampus; Human; Laminar electrophysiology; Histology; CA1; DG; Interictal spike; Bursting unit

Introduction

Temporal lobe epilepsy (TLE) is a devastating disease, causing cognitive impairment and decreased quality of life.

The hippocampus plays a central role in the generation and maintenance of the paroxysmal activity in TLE. Numerous morphological and in vivo electrophysiological studies have assessed the structural and functional disturbances in the human hippocampus caused by TLE; however, these studies lack accurate co-registration of histology and electrophysiology. We believe that co-registration of the in vivo functional and morphological findings is a very important issue to elucidate the anatomical sources and network bases of

* Corresponding author. Department of Psychophysiology, Institute for Psychology of the Hungarian Academy of Sciences, Szondi u. 83-85, Budapest 1068, Hungary. Fax: +36-1-354-2416.

E-mail address: ulbert@cogpsyphy.hu (I. Ulbert).

paroxysmal events, and define the functional connections between the closely spaced structures of the human hippocampus.

In the last two decades, powerful electrophysiological techniques have been developed to reveal the network interactions of the rodent hippocampus in vivo (Csicsvari et al., 2003). Silicone probes were implanted chronically mostly into rats, and a significant amount of information has been collected during several tasks, various stages of vigilance, and induced seizures (Bragin et al., 1997, 2002a). Laminar field potentials recorded from the hippocampus yield information about its synaptic and cellular properties (Buzsaki et al., 1986). Multiple, single unit activity (MUA, SUA) and current source density (CSD) analysis (Freeman and Nicholson, 1975; Nicholson and Freeman, 1975) have been developed and utilized to investigate hippocampal circuitry. Together with histological co-registration, CSD and MUA can identify the micro-anatomical sources of postsynaptic currents and spiking activity (Bragin et al., 1997, 2000). However, the morphology and the connections of the human hippocampus are more complex than in rodents (Lim et al., 1997a,b), consequently their electrophysiological properties may also seem different. As an example, it is still debated whether the classically defined theta oscillation—a fundamental electrographic element of the rodent hippocampal activity—exists at all in the human hippocampus (Bodizs et al., 2001; Caplan et al., 2003; Halgren, 1991; Kahana et al., 2001; O'Keefe and Burgess, 1999).

In epileptic humans, together with the clinical depth electrodes, microwires (Babb et al., 1973; Halgren et al., 1978; Staba et al., 2002a,b; Wyler et al., 1982) were implanted to record neuronal activity from the hippocampus. These devices were not designed to resolve the laminar potential profile to produce CSD traces and spatially dense laminar information about action potential spiking activity (MUA, SUA). To record laminar field potentials and MUA, SUA, multicontact linear array electrodes with 500 μm spacing were implemented (Bragin et al., 2002b), but these devices are still not optimal for the CSD analysis. Another shortcoming of the above methods is the uncertainty of electrode tip localization. MR scans were used to define the electrode coordinates, but MR has a limited resolution and often considerable spatial distortion. Moreover, the hippocampus could not be recovered after resection to verify the location of the electrode track and to investigate the degree of structural reorganization in the vicinity of the electrophysiological recordings.

Here we present a combined approach that allows recording of laminar field potentials and spiking activity together with identification of the microanatomy at the recording sites in the hippocampus of epileptic patients undergoing temporal lobectomy. In addition, the methodology yields very important information about the reorganization of the hippocampus surrounding the electrode track via immunohistochemical techniques. Examples of laminar field potential and

MUA, SUA traces from various depths of the hippocampus will be presented, together with the histological/immunohistochemical analysis. With the aid of this technique, we can have a better insight into the functional and structural properties of the hippocampal involvement in TLE.

Methods

A crucial aspect of this investigation is the coordination among neurosurgery, electrophysiology, and histology. Patients who participated in this research all underwent temporal lobectomy (hippocampectomy) as treatment for long-standing medically intractable TLE. Each subject was fully informed and consented under the auspices of the Hungarian Medical Research Council, in accordance with the Declaration of Helsinki. Intraoperative recordings were only done in the hippocampus and in the middle temporal gyrus (T2) to be resected, thus no additional risks that may stem from the invasive nature of our investigation were anticipated.

Electrophysiology and surgery

Laminar multicontact microelectrodes (multielectrodes, ME) were designed for animals with a long shaft to reach deep structures in the brain (Barna et al., 1981; Mehta et al., 2000a,b). In a previous paper (Ulbert et al., 2001a), thumb-tack MEs (tME) were introduced to sample cortical structures (Ulbert et al., 2001b) from humans. These MEs were not adequate for quick intraoperative hippocampal insertion, so they were redesigned to minimize the additional time needed to mount the device and record during the surgery.

The depth ME (dME) is manufactured the same way as the tME (Ulbert et al., 2001a). The recent design is a 10-cm-long, 350- μm -diameter, stainless steel shaft, sharp tip device, with 24 contacts, formed by the cut end of 25- μm -diameter Pt/Ir wires, center-to-center distance is 100 μm (Fig. 1A). To mount the dME, it was glued on a precision small sledge with epoxy, which was then attached to a micromanipulator with a screw lock system, so it could be roughly positioned before the insertion. The micromanipulator was equipped with a precision dial advancing mechanism and a measure, so the depth of the penetration could be controlled with 100 μm accuracy after securing the rough positioning screw. All the equipment, preamplifiers and cables going into the surgical field were sterilized in ethylene oxide. The micromanipulator was mounted on a medical instrument holder during surgery, which could be fixed in position and allowed the surgeon to aim toward the hippocampus. Under visual control using an operating microscope, the electrode tip was advanced into the hippocampus after temporal pole resection. The pole resection was done under general anesthesia (Fentanyl, Diprivan and N_2O or Isofluran or Sevofluran and N_2O) from a small craniotomy (3–5 cm) to reveal the head and the initial part of

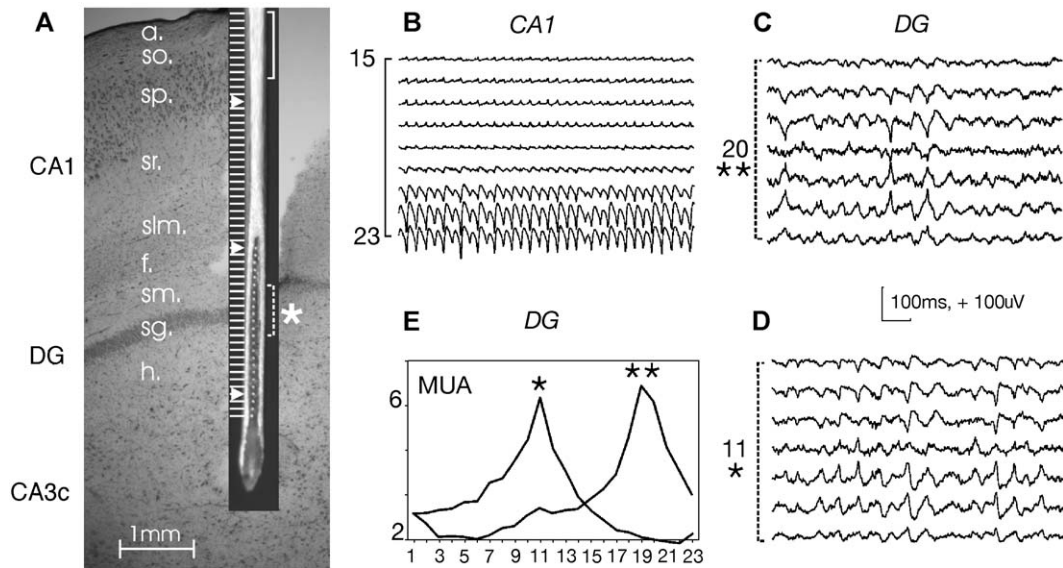


Fig. 1. (A) Reconstruction of pt.1 electrode track with the dME superimposed. Calibration bar: 1 mm, 60- μ m-thick Nissl-stained section. The photomicrograph of the dME was inserted in the slide to illustrate its position in the hippocampus. DG: dentate gyrus, a.: alveus, so.: stratum oriens, sp.: stratum pyramidale, sr.: stratum radiatum, slm.: stratum lacunosum-moleculare, f.: fissura hippocampi, sm.: stratum moleculare of the DG, sg.: stratum granulosum, h.: hilus. White grating (100 μ m apart) on the side of the dME indicates the depth of the recording sites, distance between arrows: 2 mm. Solid white bracket refers to the location of the field potential gradient shown in B (solid black bracket), dashed white bracket refers to the location of the field potential gradient shown in C and D (dashed black brackets). Double black asterisks denote the sg. in the first electrode position, while single black asterisk denotes sg. in the second electrode position, when the dME was lowered by 1 mm. A shows the approximate location of the dME in the tissue, in the second (lowered 1 mm) electrode position. (B) Injury potentials from the CA1 subfield. Representative single sweep PG traces show oscillatory activity after the dME entered the hippocampus for the first time. The oscillation lasted only for about 60 s, and then diminished. No single unit spikes were detected. Note that PG is positive in so. and inverts rapidly in sp., the same profile is apparent in Fig. 2B (CA1) with nearly identical inversion depth. Calibration: 100 ms, +100 μ V, positive potentials are depicted upwards in all of the figures. (C and D) Oscillatory activity in DG while the manipulator was moved down with \sim 1 mm, representative traces. C was recorded before the movement, the PG inversion is at channel 20 (marked with **), after the movement PG inversion slides to channel 11 (marked with *), accounting for \sim 1 mm displacement of the dME in the tissue. (E) The depth profile of the ongoing MUA averaged during a 1-min period before and after repositioning the dME. X-axis: channel numbers, Y-axis intensity, arbitrary units. Note that the MUA peak moved from channel 19–20 to channel 11, as the zero zone on C and D.

the body of the hippocampus, which is a routine approach for hippocampectomy. After positioning onto the hippocampal surface, the electrode was advanced into the hippocampus with 2-mm increments. At each 2-mm step, we recorded for 2–5 min continuously. One or two penetrations were made, usually crossing the CA1, dentate gyrus (DG), hilus, and CA3c. Spatial field potential gradient (PG, first spatial derivative of the laminar field potentials) was collected in the low-frequency band (EEG; 0.1–500 Hz, sampled at 2 kHz/channel, 16 bit) and high-frequency band (MUA; 150–5000 Hz, sampled at 20 kHz/channel, 12 bit) simultaneously. In two patients, intraoperative electrocorticography (ECoG), and in one patient intracortical tME observations were performed. Details about the amplifier and acquisition system were published previously (Ulbert et al., 2001a).

After the recordings were done, the dME was pulled out, and the hippocampus was resected en bloc. The neurosurgeon and the histologist confirmed and recorded the region and angle of the electrode insertion based on the surface vascularization of the hippocampus, because the entrance point of the dME was sometimes not apparent. Digital photograph was taken of the removed hippocampal part, and then the block was cut into 4- to 5-mm-thick slabs in the

operating room, parallel with the electrode trajectory. Another photograph was taken of the cut slab containing the electrode track, it was measured to allow subsequent estimation of shrinkage, and finally all of the slabs were put into fixative separately.

Histology, immunohistochemistry

The fixative contained 4% paraformaldehyde, 0.05% glutaraldehyde, and 0.2% picric acid in 0.1 M phosphate buffer (PB, pH = 7.4), it was hourly changed to a fresh solution during constant agitation for 6 h, and then the blocks were postfixed in the same solution overnight. Vibratome sections (60 μ m thick) were cut from the blocks, and following washing in PB, they were immersed in 30% sucrose for 1–2 days, and then frozen three times over liquid nitrogen.

Sections were processed for immunostaining as follows: They were transferred to TRIS-buffered saline (TBS, pH = 7.4), and then endogenous peroxidase activity was blocked by 1% H₂O₂ in TBS for 10 min. TBS was used for all the washes (3 \times 10 min between each antiserum) and for dilution of the antisera. Nonspecific immunostaining was blocked by

5% milk powder and 2% bovine serum albumin. A polyclonal rabbit antiserum against glutamate receptor 2 and 3 subunit (GluR2/3, 1:100, Chemicon, Temecula) was used to label the principal cells for 2 days at 4°C. For the visualization of immunopositive elements, biotinylated anti-rabbit IgG (1:250, Vector) was applied as secondary serum followed by avidin–biotinylated horseradish peroxidase complex (ABC, 1:250, Vector). The immunoperoxidase reaction was developed by 3,3'-diaminobenzidine tetrahydrochloride (DAB, Sigma) as a chromogene dissolved in TRIS buffer (TB, pH = 7.6). Sections were then treated with 1% OsO₄ in PB for 40 min, dehydrated in ethanol (1% uranyl acetate was added at the 70% ethanol stage for 40 min) and mounted in Durcupan (ACM, Fluka). The specificity of the antiserum has been thoroughly tested by the laboratory of origin.

Controls of the method included the incubation of sections in the same way, but primary antisera were replaced by the respective normal sera. No specific immunostaining could be detected under these conditions. Alternate sections (every sixth) were mounted from gelatin, and processed for cresyl violet (Nissl) staining, air-dried, dehydrated in xylene, and covered with Depex neutral medium for identification of the electrode track. Control hippocampal tissue was obtained from two patients, who died by accident, with no neurological disorder (Magloczky et al., 2000).

Results

Eleven patients were implanted with the dME. We recovered the full electrode track in six patients, while parts of the track were found in five patients. From all of the patients, we were able to obtain electrophysiology data. Complete co-registration of the electrophysiology with the histology was done in four patients. In three out of the four co-registered patients, the electrode track was found in the CA1/DG/CA3 axis, in the remaining co-registered patient, the electrode track was from CA1/CA1i (internal digitations). Two out of the four patients with fully reconstructed electrode track had a well-preserved CA1 region with numerous pyramidal cells, while the other subjects showed hippocampal sclerosis with moderate to massive CA1 pyramidal cell loss and gliosis. Here we present histological and electrophysiological data from the CA1 and DG of the two nonsclerotic hippocampi (left side). Both patients were anesthetized with N₂O, Diprivan (propofol), and Fentanyl.

Patient 1 (pt.1, male, age 14, right handed) had complex partial seizures (CPS) since age of 4, seizure frequency of 6–20 per week, localized left temporal EEG seizure onset, severe bilateral temporal mental status, left temporal medio-basal dysgenesis on the MR. After the surgery, this patient remained seizure-free with highly recovered cognitive status (improved memory and social skills) at 9 months follow up. The electrode was placed in the posterior part of the hippocampal head with CA1, DG, hilus, CA3c trajectory

(Fig. 1A), where it crossed the principal cell layers close to perpendicular in the coronal plane.

Patient 2 (pt.2, male, age 46, right handed) had 8 years history of CPS, seizure frequency was 1 per week, EEG showed left fronto-temporal seizure onset, no significant MR findings. After the surgery, one seizure was detected at 6 months follow up. The electrode was placed in the hippocampal digitations, with CA1, CA1i (internal digitations) trajectory (Fig. 2A), in addition, intracortical recordings in T2 were also made before removing the temporal pole (Figs. 2C, E).

GluR2/3 is known to be present predominantly in principal cells of the human hippocampus (de Lanerolle et al., 1998). GluR2/3 immunocytochemistry and cresyl violet staining were used to identify the exact hippocampal regions containing the electrode track and the pattern of principal cell loss. Hippocampal regions were identified in coronal sections according to Duvernoy (1998) and Amaral and Insausti (1990).

Co-registration and verification

Co-registration of the electrophysiological data with the anatomical structures was done on the 60- μ m-thick Nissl-stained sections showing the longest electrode track to minimize distortion stemming from the deviation of the trajectory and the cutting angle (Fig. 1A). Here we show the detailed procedure in pt.1 with CA1, DG, hilus trajectory. The measured tissue shrinkage was about 30%. The best section was digitized at high resolution with distance calibration and transferred into CorelDraw (Corel Inc., Dallas, TX), an accurate vector graphics software, to reconstruct the electrode tract and potential profile corresponding to the individual recording sites and epochs. Using the 30% shrinkage value, the readings from the micromanipulator and additional information from the height of the first penetration (tracked by the operating microscope), all the spatial positions of the recording epochs were marked on the digitized slide (Fig. 1A). We acquired separate files for each movement of the dME. Figs. 1B and 2B show the PG profile after the first 2-mm penetration into the hippocampus. The profiles are quite similar, which—together with the similar positions of the two CA1s derived from histology—suggests uniform initial insertion. The acquisition started before the movement, so we could compare the electrical activity before and after advancing the electrode. The result of the graphical co-registration procedure was then combined with the electrophysiology. Samples of single sweep electrical activity were displayed on the side of the graphical co-registration depicting all the channels in the corresponding depth of each recording site (as illustrated in Fig. 1).

On the basis of the graphical co-registration, in all of the patients, where the dME penetrated the DG ($n = 6$), a typical sharply contoured oscillatory activity was observed on the electrode sites falling in the region of the DG. Depending on the penetrating angle and thickness of the granule cell layer

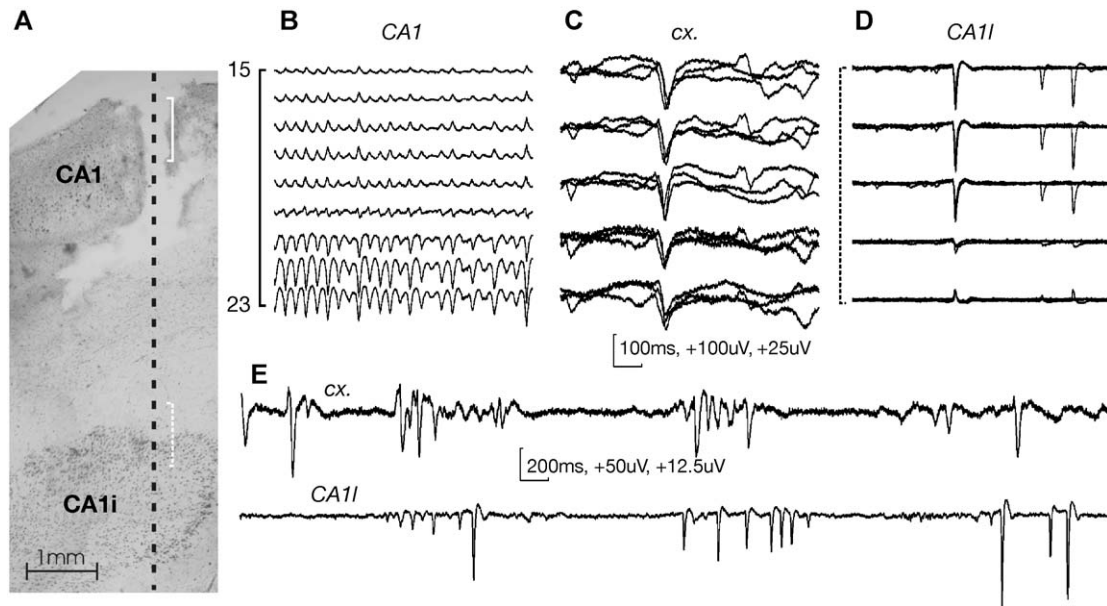


Fig. 2. (A) Reconstructive montage of pt.2. CA1 and CA1i in the hippocampal digitations. Nissl-stained, 60- μ m-thick section, calibration bar: 1 mm. Slightly oblique section, the track is only visible in CA1. Dashed line indicates the continuation of the penetration that crosses CA1i nearly parallel with the axis of the pyramidal cells. Solid bracket refers to the CA1, dashed bracket refers to the CA1i recording. (B) Injury potentials from CA1. Identical to Fig. 1B. Note that the inversion is nearly at the same channel as in Fig. 1B, the shape and frequency of the activity is quite similar too. Calibration: 100 ms, +100 μ V. (C) Interictal spikes collected before temporal pole resection from the middle temporal gyrus (T2). Recordings from layers II to III, three representative single sweeps are superimposed. The tMEs were implanted for 10 min to record temporal cortex spikes, to test if hippocampal activity after pole resection has common patterns with T2. Calibration: 100 ms, +25 μ V. (D) Interictal spikes from CA1i. Representative traces recorded close to the sp. Three sweeps superimposed. The spike latency is shorter than in T2, and the morphology of the separate spikes has much less variation, than in T2. Every second channel is shown. Calibration: 100 ms, +100 μ V. (E) Long time scale plots of T2 (upper trace) and CA1i (lower trace) activity. Similar timing of single spikes and polyspike trains in T2 and CA1i suggesting common generator mechanisms; however, the intracortical activity is slower and shows larger variation, suggesting cortical network modulation of epileptic discharges. Calibration: 100 ms, +50 μ V for the CA1i; 100 ms, +12.5 μ V for the cortex.

(stratum granulosum: sg.), an abrupt potential inversion (Figs. 1C, D) and a highly localized spatial MUA profile (Fig. 1E) was apparent. This way, sg. served as a natural landmark allowing us to verify the graphical co-registration. Granule cells are known to generate oscillatory synaptic and spiking activity in the rat under epileptogenic conditions (Cohen et al., 2003; Kobayashi and Buckmaster, 2003; Towers et al., 2002). Earlier data indicated that the human DG can also produce this type of population discharge pattern (Williamson et al., 1995a,b). Because MUA is generated by the discharge of neurons surrounding the electrode contacts, it is most pronounced around the cell body layer, and decays rapidly with distance. Thus, comparing the depth of the maximal spiking activity with the location of the sg. would give us a good measure to verify the graphical co-registration procedure, because (i) the sg. of the human DG is easily identified in the Nissl-stained sections (Fig. 1A), (ii) it is quite thin (about 200 μ m) in contrast to the CA1 pyramidal layer (stratum pyramidale: sp.), and (iii) no other dense cell layer is located around it.

To test the relative movement of the dME in the tissue, we constructed the spatial amplitude profile of the spiking activity via averaging the ongoing MUA (Ulbert et al., 2001a,b) in a 1-min interval in two consecutive epochs, recorded 1 mm apart from each other (Fig. 1E) as indexed by the reading on the microdrive. As the dME moved 1 mm

downward, the MUA maximum shifted about 1 mm too. The PG inversion (compare Figs. 1C and D) showed a similar shift, providing additional evidence that the relative movement is accurate. The same measures were used to define absolute error of the co-registration process. While moving the dME by 6 mm, the maximal MUA fell within the sg. of the DG (Figs. 1A, E), indicating that our graphical co-registration procedure had less than 200 μ m error during total electrode movement, which is consistent with a \sim 4% gross localization error. The position of the potential inversion (zero zone) was concordant with the above findings (Figs. 1C, D), strengthening the accuracy of our localization procedure.

Stability of the recordings

Displacement of the ME against the tissue could stem from two sources. The first is the instability of the microdrive: it can slowly drift down because of the weight of the ME, preamplifier, and cabling. The second is the movement of the tissue: rebound from the initial deformation of the insertion. Because this kind of movement could be very small, it would be extremely hard to detect in an intraoperative setting, based only on physical distance measurements. Good physiological localization information can be drawn from the spatial pattern of the SUA. In vivo hippocampal recordings in rats with 25 μ m

intercontact spacing laminar electrodes (Henze et al., 2000) showed a rapidly changing spatial action potential profile of CA1 pyramidal cells. A 50- μm displacement parallel with the axis of the pyramidal cell could reduce the action potential peak measured at a given site by as much as 40%. Here we measured the changes of the peak action potential amplitude of a CA1 (Figs. 2A and 3) presumably pyramidal cell during a 4-min recording session in pt.2. As seen in Fig. 3B, the peak decrement was less than 20%, which translates to an electrode shift smaller than 50 μm .

Injury-related potentials and effects of anesthesia

In patients where CA1 pyramids were preserved in the vicinity of the electrode track ($n = 2$), a characteristic fast and sharp oscillation occurred after the first penetration (compare Figs. 1A, B and 2A, B), which faded usually in 1 min. The frequency started at about 30–40 Hz and gradually decreased together with the peak amplitude, until it vanished. The DG ($n = 6$) showed similar sharp oscillation (40–50 Hz), which was faster and larger during the first 1 min of recording immediately after penetrating the granule cell layer. The spatial PG and MUA distribution of this oscillation was the same before and after the frequency stabilized to 8–18 Hz (Figs. 1C, D), and this ongoing spatial distribution did not change for the rest of the recordings (more than 5 min), suggesting intrinsic rather than injury-related activity.

In two patients, subdural strip recordings were performed before the depth observations and in pt.2 we implanted a tME in the medial temporal gyrus (Fig. 2E upper trace, long time scale) before temporal pole resection, and before the

hippocampal recordings (Fig. 2E lower trace, long time scale). In all of these cases, frequent interictal spiking was apparent both in the cortex and the hippocampus, suggesting the preservation of active epileptic processes in these patients under anesthesia.

In pt.2, where both tME and dME were implanted (albeit not simultaneously), we measured the mean recurrence frequency of single interictal spikes for the hippocampus (hc.): 1.3 ± 0.4 Hz and cortex (cx.): 1 ± 0.3 Hz, $n = 25$, the mean latency between individual spikes in polyspike trains in hc.: 89.2 ± 25.5 ms and cx.: 116.8 ± 48.1 ms, $n = 50$, and mean onset to peak spike latency of hc.: 9.73 ± 1.7 ms and cx.: 19.6 ± 3.9 ms, $n = 25$, to characterize cortical (T2) and hippocampal activity. Interictal spikes were selected by the neurologist with a custom Matlab (The MathWorks Inc., Natick, MA) code, based on peak detection. Polyspike trains were defined based on interspike interval criteria. If an initial spike was followed by at least one spike in less than 300 ms, it was regarded as a polyspike train. Onset to peak latency was defined as the time needed for the spike to reach from 10% to maximum peak amplitude, baseline was calculated from the 75- to 50-ms interval before the spike peak. Individual short time scale traces from cortex (supragranular layers) and hippocampus (CA1i) are presented in Figs. 2C and D. The similarity of their shape and temporal recurrence pattern (see also Fig. 2E) suggests, that these large field potential spikes reflect epileptic network activity, rather than injury-related potentials. It is also notable, that the single unit bursting activity showed close relationship with the field potential spikes in CA1i (Fig. 3D), 85% of the bursts happened on the descending part of the spikes, suggesting synaptic and cellular coupling in certain parts of the hippocampus.

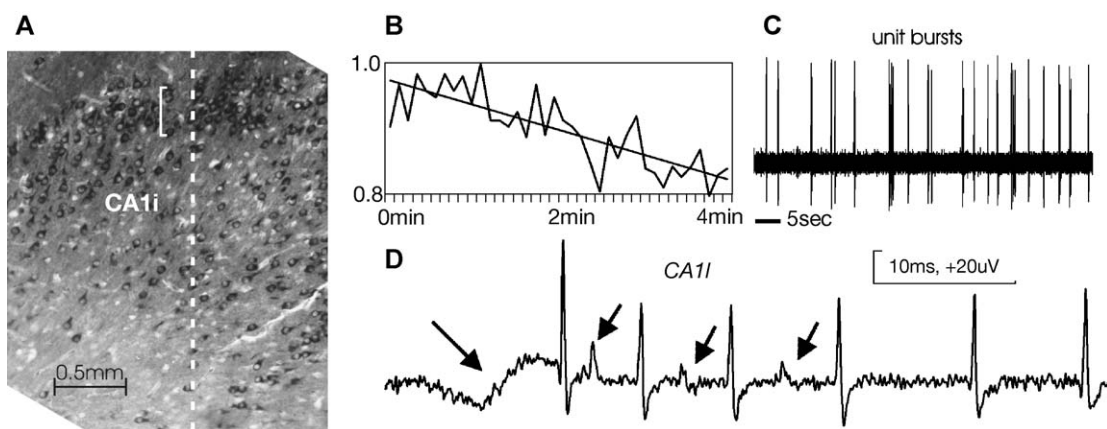


Fig. 3. (A) GluR2/3 stain of pt.2 CA1i region. Calibration bar: 500 μm , white bracket shows the approximate location of the bursting putative pyramidal cell. Dashed white line indicates the electrode track, which was located approximately 250–300 μm from this section. Note the dense cell body layer which is nearly perpendicular to the electrode trajectory. (B) Peak amplitude change of a bursting unit. Normalized peak amplitude of the first firing of a burst is plotted against recording time. The figure indicates less than 20% change during the 4-min interval. (C) Unit recordings from CA1i. This figure shows the stability of the unit recordings with very good signal-to-noise ratio. (D) Burst discharges. One putative pyramidal neuron (corresponds to the location marked with the white bracket in A) exhibits prolonged bursting (5–10 spikes at ~ 150 –100 Hz) at the descending part of the large field potential spike. Raw waveform, note that positivity is up, since we used differential recording (PG). Long arrow points on the preceding interictal spike peak. Small arrows point to the interdigitating firing of another neuron. This pattern was observed very frequently during the recording. Calibration: 10 ms, +20 μV .

Discussion

A depth laminar multielectrode system and surgical positioning device have been developed, optimized for intraoperative electrophysiological observations, and combined with histology/reconstruction techniques for co-registration with the hippocampal micro-anatomy. The spatial stability, accuracy of the recording apparatus, and co-registration of functional and morphological data were tested and verified successfully.

Despite of the ongoing debate on acute monitoring during epilepsy surgery (Tran et al., 1995), intraoperative ECoG and/or direct hippocampal recordings are used, to localize epileptic network activity, and to tailor focus resection (Alarcon et al., 1997; McKhann et al., 2000; Polkey et al., 1989). These studies were conducted under general anesthesia, in an acute setting, similar to our observations, and their results confirmed that intraoperative ECoG and/or hippocampal recordings can be useful diagnostic tools in certain cases. In our opinion, outcome and long-term follow up could serve, at least as a partial substitute for the direct electrophysiological control, though we do not have direct evidences that some effect of injury can be ruled out. Nitrous oxide does not modify interictal spiking during intraoperative ECoG (Hosain et al., 1997), fentanyl (and its derivatives) is rather a specific agent to assist focus localization during surgery (Manninen et al., 1999; McGuire et al., 2003), while propofol showed no sign of intrinsic epileptogenicity in a sleep study (Leijten et al., 2001), its effect on intraoperative spiking was significant, but did not interfere with the ECoG interpretation (Herrick et al., 1997). Though it was not explicitly tested in here, it is feasible, that the anesthesia used, had no major nonspecific epileptogenic effect. Also the outcomes of the surgeries were favorable, suggesting that the structures examined (and then resected) might have been involved in the network, generating paroxysmal events.

During the experiments we experienced no bleeding or other complications, and no post-surgery neurological deficits of any kind occurred due to the electrode implantations. We have found several different patterns of hippocampal activation, such as pyramidal cell bursting, large field potential spikes originating in CA1, and rhythmic activity both in the DG and CA1.

Cellular bursting in the epileptic hippocampus was observed in vivo during waking, slow wave, and paradoxical sleep (Colder et al., 1996; Ravagnati et al., 1979; Staba et al., 2002b). Here we demonstrated that CA1i pyramidal bursting activity can be detected under anesthesia (Fig. 3).

We could identify hippocampal locations with about $\pm 100 \mu\text{m}$ error, which exceeds the MRI localization accuracy. This allowed us to determine the anatomical structure, where the bursting cell was located (CA1i in this case). Because immunohistochemistry reveals the fine structure of the surrounding tissue, including the degree of cell loss and

reorganization, this technique puts the electrophysiological information into a structural context.

Large field potential spikes occur in the subiculum (Cohen et al., 2002), and other regions of the limbic system (Babb et al., 1987; Wyler et al., 1982). Here we demonstrated, for the first time, similar activity in the histologically identified human CA1i under anesthesia. The CA1i spike waveforms (Figs. 2D, E) from our experiments are quite similar to the in vitro subicular ones suggesting similar mechanisms underlying the epileptic discharges. Intracortical recordings from T2 before temporal pole resection revealed similar temporal spiking patterns and spike morphology as recorded from the CA1i after temporal pole resection in pt.2 (Fig. 2E). This result is in accordance with the findings of Cohen et al. (2002), implicating functional connections between the CA1-subicular region and lateral temporal structures.

In addition, the nonsclerotic CA1 produced transient injury-related potentials, which were remarkably similar among patients, suggesting homologous generator mechanisms and elevated CA1 excitability. Though this rhythmic pattern faded rapidly, its underlying mechanisms could participate in the epileptic network activity.

In TLE, the main mass of the DG is preserved (Margerison and Corsellis, 1966). DG cells contribute to epileptic reorganization via mossy fiber sprouting (Sutula et al., 1989). Various findings indicate that the DG is heavily involved in the generation and maintenance of paroxysmal activity in TLE, because of the reorganization/imbalance of its inhibitory and/or excitatory circuits (Isokawa-Akesson et al., 1989; Magloczky et al., 2000; Prince and Jacobs, 1998; Williamson et al., 1995b, 1999; Wittner et al., 2001). Until now, no in vivo electrophysiological recordings were obtained from anatomically identified laminae of the human DG. We have found sharp, rhythmic field potential oscillations and elevated cellular spiking activity originating in the DG under anesthesia. The spatial extent of the PG activity was confined to a 500- to 600- μm -wide region coinciding with the DG, while the MUA fell even more rapidly in space, allowing us to define the granule cell layer as an electrophysiological landmark in most of the patients implanted (Fig. 1). Whether this oscillatory DG activity in humans reflects its normal gating mechanism, or it is a consequence of build-up of recurrent excitation caused by mossy fiber sprouting (Buckmaster et al., 2002), cannot be answered solely from these observations, mostly because the dimensions of the electrode did not allow us to record from other structures simultaneously to test their interactions. Given the large size of the human hippocampus, if we want to record—for example—from CA1 and DG simultaneously, either we have to increase the intercontact spacing or use two or more dMEs. To further examine the effect of anesthesia and injury, the authors are planning to design new electrodes, which are suitable to record chronically from the implanted, awake patients.

These observations indicate that there is a high degree of preserved hippocampal and temporal cortex activity in anesthetized humans with TLE. Large-scale network connections might also be in operation under these conditions, allowing the experimenter to investigate the medial and lateral temporal lobe interactions. Similarity of local electrophysiological patterns across patients in CA1 and also in DG further strengthens our conclusion that intraoperative observations of electrical activity patterns, together with appropriate post hoc identification of the precise anatomical sites of their origin, could further enhance our knowledge about the differential and specific involvement of hippocampal subfields in TLE.

Acknowledgments

This work was supported in part by: EUM (ETT442-04), OTKA (T032251), NIH (NS18741, NS44623), NIH (MH54671), and the Howard Hughes Medical Institute. We thank Dr. György Kollár and Dr. András Fogarasi for their neurological support and László Papp for his technical support.

References

- Alarcon, G., Garcia Seoane, J.J., Binnie, C.D., Martin Miguel, M.C., Juler, J., Polkey, C.E., Elwes, R.D., Ortiz Blasco, J.M., 1997. Origin and propagation of interictal discharges in the acute electrocorticogram. Implications for pathophysiology and surgical treatment of temporal lobe epilepsy. *Brain* 120 (Pt 12), 2259–2282.
- Amaral, D.G., Insausti, R., 1990. *Hippocampal Formation*. Academic Press, New York.
- Babb, T.L., Carr, E., Crandall, P.H., 1973. Analysis of extracellular firing patterns of deep temporal lobe structures in man. *Electroencephalogr. Clin. Neurophysiol.* 34, 247–257.
- Babb, T.L., Wilson, C.L., Isokawa-Akesson, M., 1987. Firing patterns of human limbic neurons during stereoencephalography (SEEG) and clinical temporal lobe seizures. *Electroencephalogr. Clin. Neurophysiol.* 66, 467–482.
- Barna, J.S., Arezzo, J.C., Vaughan Jr., H.G., 1981. A new multielectrode array for the simultaneous recording of field potentials and unit activity. *Electroencephalogr. Clin. Neurophysiol.* 52, 494–496.
- Bodizs, R., Kantor, S., Szabo, G., Szucs, A., Eross, L., Halasz, P., 2001. Rhythmic hippocampal slow oscillation characterizes REM sleep in humans. *Hippocampus* 11, 747–753.
- Bragin, A., Csicsvari, J., Penttonen, M., Buzsaki, G., 1997. Epileptic after-discharge in the hippocampal–entorhinal system: current source density and unit studies. *Neuroscience* 76, 1187–1203.
- Bragin, A., Hetke, J., Wilson, C.L., Anderson, D.J., Engel Jr., J., Buzsaki, G., 2000. Multiple site silicon-based probes for chronic recordings in freely moving rats: implantation, recording and histological verification. *J. Neurosci. Methods* 98, 77–82.
- Bragin, A., Wilson, C.L., Engel Jr., J., 2002a. Rate of interictal events and spontaneous seizures in epileptic rats after electrical stimulation of hippocampus and its afferents. *Epilepsia* 43 (Suppl. 5), 81–85.
- Bragin, A., Wilson, C.L., Staba, R.J., Reddick, M., Fried, I., Engel Jr., J., 2002b. Interictal high-frequency oscillations (80–500 Hz) in the human epileptic brain: entorhinal cortex. *Ann. Neurol.* 52, 407–415.
- Buckmaster, P.S., Zhang, G.F., Yamawaki, R., 2002. Axon sprouting in a model of temporal lobe epilepsy creates a predominantly excitatory feedback circuit. *J. Neurosci.* 22, 6650–6658.
- Buzsaki, G., Czopf, J., Kondakor, I., Kellenyi, L., 1986. Laminar distribution of hippocampal rhythmic slow activity (RSA) in the behaving rat: current-source density analysis, effects of urethane and atropine. *Brain Res.* 365, 125–137.
- Caplan, J.B., Madsen, J.R., Schulze-Bonhage, A., Aschenbrenner-Scheibe, R., Newman, E.L., Kahana, M.J., 2003. Human theta oscillations related to sensorimotor integration and spatial learning. *J. Neurosci.* 23, 4726–4736.
- Cohen, I., Navarro, V., Clemenceau, S., Baulac, M., Miles, R., 2002. On the origin of interictal activity in human temporal lobe epilepsy in vitro. *Science* 298, 1418–1421.
- Cohen, A.S., Lin, D.D., Quirk, G.L., Coulter, D.A., 2003. Dentate granule cell GABA(A) receptors in epileptic hippocampus: enhanced synaptic efficacy and altered pharmacology. *Eur. J. Neurosci.* 17, 1607–1616.
- Colder, B.W., Wilson, C.L., Frysinger, R.C., Chao, L.C., Harper, R.M., Engel Jr., J., 1996. Neuronal synchrony in relation to burst discharge in epileptic human temporal lobes. *J. Neurophysiol.* 75, 2496–2508.
- Csicsvari, J., Jamieson, B., Wise, K.D., Buzsaki, G., 2003. Mechanisms of gamma oscillations in the hippocampus of the behaving rat. *Neuron* 37, 311–322.
- de Lanerolle, N.C., Eid, T., von Campe, G., Kovacs, I., Spencer, D.D., Brines, M., 1998. Glutamate receptor subunits GluR1 and GluR2/3 distribution shows reorganization in the human epileptogenic hippocampus. *Eur. J. Neurosci.* 10, 1687–1703.
- Duvernoy, H.M., 1998. *The Human Hippocampus*. Springer-Verlag, Berlin.
- Freeman, J.A., Nicholson, C., 1975. Experimental optimization of current source-density technique for anuran cerebellum. *J. Neurophysiol.* 38, 369–382.
- Halgren, E., 1991. Firing of human hippocampal units in relation to voluntary movements. *Hippocampus* 1, 153–161.
- Halgren, E., Babb, T.L., Crandall, P.H., 1978. Activity of human hippocampal formation and amygdala neurons during memory testing. *Electroencephalogr. Clin. Neurophysiol.* 45, 585–601.
- Henze, D.A., Borhegyi, Z., Csicsvari, J., Mamiya, A., Harris, K.D., Buzsaki, G., 2000. Intracellular features predicted by extracellular recordings in the hippocampus in vivo. *J. Neurophysiol.* 84, 390–400.
- Herrick, I.A., Craen, R.A., Gelb, A.W., McLachlan, R.S., Girvin, J.P., Parrent, A.G., Eliasziw, M., Kirkby, J., 1997. Propofol sedation during awake craniotomy for seizures: electrocorticographic and epileptogenic effects. *Anesth. Analg.* 84, 1280–1284.
- Hosain, S., Nagarajan, L., Fraser, R., Van Poznak, A., Labar, D., 1997. Effects of nitrous oxide on electrocorticography during epilepsy surgery. *Electroencephalogr. Clin. Neurophysiol.* 102, 340–342.
- Isokawa-Akesson, M., Wilson, C.L., Babb, T.L., 1989. Inhibition in synchronously firing human hippocampal neurons. *Epilepsy Res.* 3, 236–247.
- Kahana, M.J., Seelig, D., Madsen, J.R., 2001. Theta returns. *Curr. Opin. Neurobiol.* 11, 739–744.
- Kobayashi, M., Buckmaster, P.S., 2003. Reduced inhibition of dentate granule cells in a model of temporal lobe epilepsy. *J. Neurosci.* 23, 2440–2452.
- Leijten, F.S., Teunissen, N.W., Wieneke, G.H., Knape, J.T., Schobben, A.F., van Huffelen, A.C., 2001. Activation of interictal spiking in mesiotemporal lobe epilepsy by propofol-induced sleep. *J. Clin. Neurophysiol.* 18, 291–298.
- Lim, C., Blume, H.W., Madsen, J.R., Saper, C.B., 1997a. Connections of the hippocampal formation in humans: I. The mossy fiber pathway. *J. Comp. Neurol.* 385, 325–351.
- Lim, C., Mufson, E.J., Kordower, J.H., Blume, H.W., Madsen, J.R., Saper, C.B., 1997b. Connections of the hippocampal formation in humans: II. The endfolial fiber pathway. *J. Comp. Neurol.* 385, 352–371.
- Magloczky, Z., Wittner, L., Borhegyi, Z., Halasz, P., Vajda, J., Czirjak, S., Freund, T.F., 2000. Changes in the distribution and connectivity of interneurons in the epileptic human dentate gyrus. *Neuroscience* 96, 7–25.

- Manninen, P.H., Burke, S.J., Wennberg, R., Lozano, A.M., El Beheiry, H., 1999. Intraoperative localization of an epileptogenic focus with alfentanil and fentanyl. *Anesth. Analg.* 88, 1101–1106.
- Margerison, J.H., Corsellis, J.A., 1966. Epilepsy and the temporal lobes. A clinical, electroencephalographic and neuropathological study of the brain in epilepsy, with particular reference to the temporal lobes. *Brain* 89, 499–530.
- McGuire, G., El-Beheiry, H., Manninen, P., Lozano, A., Wennberg, R., 2003. Activation of electrocorticographic activity with remifentanyl and alfentanil during neurosurgical excision of epileptogenic focus. *Br. J. Anaesth.* 91, 651–655.
- McKhann II, G.M., Schoenfeld-McNeill, J., Born, D.E., Haglund, M.M., Ojemann, G.A., 2000. Intraoperative hippocampal electrocorticography to predict the extent of hippocampal resection in temporal lobe epilepsy surgery. *J. Neurosurg.* 93, 44–52.
- Mehta, A.D., Ulbert, I., Schroeder, C.E., 2000a. Intermodal selective attention in monkeys. I: Distribution and timing of effects across visual areas. *Cereb. Cortex* 10, 343–358.
- Mehta, A.D., Ulbert, I., Schroeder, C.E., 2000b. Intermodal selective attention in monkeys. II: Physiological mechanisms of modulation. *Cereb. Cortex* 10, 359–370.
- Nicholson, C., Freeman, J.A., 1975. Theory of current source-density analysis and determination of conductivity tensor for anuran cerebellum. *J. Neurophysiol.* 38, 356–368.
- O'Keefe, J., Burgess, N., 1999. Theta activity, virtual navigation and the human hippocampus. *Trends Cogn. Sci.* 3, 403–406.
- Polkey, C.E., Binnie, C.D., Janota, I., 1989. Acute hippocampal recording and pathology at temporal lobe resection and amygdalo-hippocampectomy for epilepsy. *J. Neurol. Neurosurg. Psychiatry* 52, 1050–1057.
- Prince, D.A., Jacobs, K., 1998. Inhibitory function in two models of chronic epileptogenesis. *Epilepsy Res.* 32, 83–92.
- Ravagnani, L., Halgren, E., Babb, T.L., Crandall, P.H., 1979. Activity of human hippocampal formation and amygdala neurons during sleep. *Sleep* 2, 161–173.
- Staba, R.J., Wilson, C.L., Bragin, A., Fried, I., Engel Jr., J., 2002a. Quantitative analysis of high-frequency oscillations (80–500 Hz) recorded in human epileptic hippocampus and entorhinal cortex. *J. Neurophysiol.* 88, 1743–1752.
- Staba, R.J., Wilson, C.L., Fried, I., Engel Jr., J., 2002b. Single neuron burst firing in the human hippocampus during sleep. *Hippocampus* 12, 724–734.
- Sutula, T., Cascino, G., Cavazos, J., Parada, I., Ramirez, L., 1989. Mossy fiber synaptic reorganization in the epileptic human temporal lobe. *Ann. Neurol.* 26, 321–330.
- Towers, S.K., LeBeau, F.E., Gloveli, T., Traub, R.D., Whittington, M.A., Buhl, E.H., 2002. Fast network oscillations in the rat dentate gyrus in vitro. *J. Neurophysiol.* 87, 1165–1168.
- Tran, T.A., Spencer, S.S., Marks, D., Javidan, M., Pacia, S., Spencer, D.D., 1995. Significance of spikes recorded on electrocorticography in non-lesional medial temporal lobe epilepsy. *Ann. Neurol.* 38, 763–770.
- Ulbert, I., Halgren, E., Heit, G., Karmos, G., 2001a. Multiple microelectrode-recording system for human intracortical applications. *J. Neurosci. Methods* 106, 69–79.
- Ulbert, I., Karmos, G., Heit, G., Halgren, E., 2001b. Early discrimination of coherent versus incoherent motion by multiunit and synaptic activity in human putative MT+. *Hum. Brain Mapp.* 13, 226–238.
- Williamson, A., Spencer, S.S., Spencer, D.D., 1995a. Depth electrode studies and intracellular dentate granule cell recordings in temporal lobe epilepsy. *Ann. Neurol.* 38, 778–787.
- Williamson, A., Telfeian, A.E., Spencer, D.D., 1995b. Prolonged GABA responses in dentate granule cells in slices isolated from patients with temporal lobe sclerosis. *J. Neurophysiol.* 74, 378–387.
- Williamson, A., Patrylo, P.R., Spencer, D.D., 1999. Decrease in inhibition in dentate granule cells from patients with medial temporal lobe epilepsy. *Ann. Neurol.* 45, 92–99.
- Wittner, L., Magloczky, Z., Borhegyi, Z., Halasz, P., Toth, S., Eross, L., Szabo, Z., Freund, T.F., 2001. Preservation of perisomatic inhibitory input of granule cells in the epileptic human dentate gyrus. *Neuroscience* 108, 587–600.
- Wyler, A.R., Ojemann, G.A., Ward Jr., A.A., 1982. Neurons in human epileptic cortex: correlation between unit and EEG activity. *Ann. Neurol.* 11, 301–308.